Applied Catalysis B: Environmental 220 (2018) 477–487

Contents lists available at ScienceDirect

Applied Catalysis B: Environmental

journal homepage: www.elsevier.com/locate/apcatb

Insights into the effects of alcohols on hydrated electron (e_{aq}^-) generation from the *p*-benzoquinone/UV process

Jia Gu[a], Ling Yang[b], Jin Jiang[a,*], Jun Ma[a,*], Wei Qiu[a], Jingxin Yang[c], Yang Song[a], Wei Quan Tian[d]

[a] State Key Laboratory of Urban Water Resource and Environment, School of Municipal and Environmental Engineering, Harbin Institute of Technology, Harbin, Heilongjiang 150090, PR China
[b] MIIT Key Laboratory of Critical Materials Technology for New Energy Conversion and Storage, School of Chemistry and Chemical Engineering, Harbin Institute of Technology, Harbin, Heilongjiang 150080 PR China
[c] School of Chemical Engineering and Technology, Sun Yat-sen University, Zhuhai 519082, PR China
[d] College of Chemistry and Chemical Engineering, Chongqing University, Chongqing 401331, PR China

ARTICLE INFO

Article history:
Received 5 May 2017
Received in revised form 21 June 2017
Accepted 11 July 2017
Available online 16 July 2017

Keywords:
p-Benzoquinone
CH_3OH
UV irradiation
Hydrated electron
Quantum chemical calculations

ABSTRACT

In this work, the effect of alcohols as hydrogen donors on hydrated electron (e_{aq}^-) generation from *p*-benzoquinone (*p*-BQ) photolysis was investigated by quantum chemical calculations and experiments to further understand the underlying mechanisms associated within the *p*-BQ/UV process. Theoretically, the UV photolysis of *p*-BQ at 253.7 nm in the presence of H_2O could induce the formation of *p*-HOC_6H_4OH and hydroxy-*p*-benzoquinone, which was almost independent of the addition of CH_3OH. While, the first triplet state of hydroxy-*p*-benzoquinone preferred to react with CH_3OH (rather than H_2O) to release the corresponding semiquinone radical and hydroxymethyl radical ($^{\bullet}CH_2OH$). These two radicals could induce the reduction of *p*-BQ to *p*-benzosemiquinone radical and thus enhanced the formation of *p*-HOC_6H_4OH as the precursor of e_{aq}^-. Experimentally, the detection of e_{aq}^- generated in the process was accomplished by the degradation of monochloroacetic acid (MCAA) (the probe of e_{aq}^-). With the addition of CH_3OH, the degradation of MCAA was accelerated in the *p*-BQ/UV process. A similar acceleration was also observed by the addition of ethanol or 2-propanol with the α-H. However, *tert*-butanol, which is without the α-H in the structure, didn't induce the acceleration. Since the quinone-like and alcoholic groups are widely distributed in the environment, these findings may improve the understanding of the photochemistry of quinones in the presence of alcohols with the α-H.

1. Introduction

Recently, advanced reduction processes (ARPs) [1] have received much attention, since ARPs can be used for the efficient remediation of polluted environments [2–6]. Especially, many studies focused on the decontamination of chlorinated [2–5] and fluorinated organic pollutants [7–11] by ARPs have been reported. The reductive degradation of halogenated organic pollutants by ARPs (i.e., the dehalogenation of chlorinated [2–5] and fluorinated pollutants [7–11]) usually leads to the conversion of the pollutants to some more environmentally benign and biodegradable products [1,12]. Some reactive species are involved in ARPs, e.g., sulfur dioxide radical ($SO_2^{\bullet-}$) [13], sulfite radical ($SO_3^{\bullet-}$) [14], hydrated electron (e_{aq}^-) [2–11], hydrogen atom ($H^{\bullet}$) [15] and excited state bisulfide ion (HS^{-*}) [16], etc.

Since its standard reduction potential is about −2.9 V [17], e_{aq}^- is one of the most reductive species, being the most suitable one for ARPs. Usually, some common inorganic reducing agents (e.g., sulfite [1–7], ferrous iron [20], and iodide [8,9,11,21]) can be the sources of e_{aq}^-. In addition, e_{aq}^- can be ejected from organic compounds (e.g., phenols [22–24] and quinones [25]).

Recently, we have confirmed that the UV photolysis of phenol at 253.7 nm in aqueous solution could induce the generation of e_{aq}^- with *p*-hydroquinone and *p*-benzoquinone (*p*-BQ) as the intermediates [24]. In the phenol/UV process, we have theoretically determined the catalysis of phenoxyl radical ($C_6H_5O^{\bullet}$) for the transformation of phenol to *p*-hydroquinone, which can help to cor-

* Corresponding authors.
E-mail addresses: jiangjin@hit.edu.cn, jiangjinhit@126.com (J. Jiang), majun@hit.edu.cn, majunhit@126.com (J. Ma).

http://dx.doi.org/10.1016/j.apcatb.2017.07.031
0926-3373/

roborate that the stoichiometric ratio of phenol to the generated e_{aq}^- was 1:4 with *p*-BQ as the product [24]. Moreover, we have also reported the generation of e_{aq}^- from the *p*-BQ/UV process in aqueous solution, with H_2O as the original source of e_{aq}^- [25]. The direct precursor of e_{aq}^- was *p*-hydroquinone, which was indicated by the dependence of the e_{aq}^- generation efficiency on pH [25]. The formation of *p*-hydroquinone in the process was via the direct triplet mechanism, which was confirmed by the DFT calculations [25]. In the process, the e_{aq}^- generation efficiency showed a positive linear dependence on the *p*-BQ concentration [25], since *p*-BQ acted as an initiator [26] and photosensitizer [27].

In the *p*-BQ/UV process, the addition of the hydrogen donor, e.g., alcohols and formate, could induce the formation of *p*-benzosemiquinone radical, which was an important intermediate for the generation of *p*-hydroquinone [28]. Thus, the hydrogen donation in the process should be investigated to improve the understanding of the e_{aq}^- generation from the UV photolysis of *p*-BQ at 253.7 nm. Görner et al. has reported that the UV photolysis of *p*-BQ at 253.7 nm in aqueous solution in the presence of CH_3OH can induce the formation of *p*-benzosemiquinone radical via the hydrogen abstraction of CH_3OH by the triplet state of *p*-BQ [28], which is the major species after pulsed excitation [26]. The UV photolysis can also lead to the simultaneous formation of hydroxymethyl radical ($^{\bullet}CH_2OH$) [28], which can cause the reduction of *p*-BQ to *p*-benzosemiquinone radical efficiently ($6.1 \times 10^9\ M^{-1}\ s^{-1}$) [29]. The generated *p*-benzosemiquinone radical can be converted to *p*-hydroquinone and *p*-BQ ($8 \times 10^7\ M^{-1}\ s^{-1}$) [30]. The formation of *p*-hydroquinone in the process [28] makes it possible to expect the generation of e_{aq}^- [27]. Obviously, CH_3OH can act as the model of alcohols to demonstrate the hydrogen donation for the e_{aq}^- generation in the *p*-BQ/UV process.

In this work, the quantum chemical calculations were carried out for the theoretical confirmation of the mechanism of the transformation in the *p*-BQ/UV process in the presence of CH_3OH. The experimental determination of enhanced e_{aq}^- generation in the process was then performed by exploring the roles of *p*-BQ, pH, and CH_3OH under various conditions. The e_{aq}^- generation efficiency was studied by the degradation of the probe of e_{aq}^-, namely recalcitrant monochloroacetic acid (MCAA) [17,31], since it can react rapidly with e_{aq}^- to release Cl^- ($1.0 \times 10^9\ M^{-1}\ s^{-1}$) [17].

2. Experimental

2.1. Materials and reagents

Most of the reagents were supplied by Sigma-Aldrich, including *p*-BQ (reagent grade, ≥98%), sodium monochloroacetate (98%), acetic acid (ACS reagent, ≥99.7%), potassium hydroxide (sigmaultra, ≥85%), sodium chloride (99.999%), sodium hydroxide (ACS reagent, ≥97.0%), sodium tetraborate decahydrate (ACS reagent, ≥99.5%), sodium phosphate dibasic (ACS reagent, ≥99.0%), sodium phosphate monobasic monohydrate (ACS reagent, 98.0–102.0%), potassium iodide (ACS reagent, ≥99.0%), potassium iodate (ACS reagent, 99.5%), ethanol (ACS reagent, ≥99.8%), 2-propanol (ACS reagent, ≥99.5%), and *tert*-butanol (ACS reagent, ≥99.0%). Methanol of HPLC grade was purchased from Fisher Chemical. Hydrogen peroxide (H_2O_2, 35% v/v, stab.) was obtained from Alfa Aesar. Without further purification, all chemicals were dissolved in ultra-pure water (18.2 MΩ cm), which was generated by the filtration of distilled water through a Millipore Milli-Q water purification system.

2.2. Experimental procedure

The photolysis experiments were conducted in a sealed reactor (V = 1000 mL), which was similar to that reported by Li et al. [2]. The UV light source in the reactor was a 15 W low-pressure mercury UV lamp (253.7 nm, ozone-free, type GPH303T5L, Light Sources). The photon flux (I_0) from the UV source to the solution, the average fluence rate (I_s) and the effective path length (L) were determined to be $(4.15 \pm 0.02) \times 10^{-6}$ einstein s^{-1}, 1.47×10^{-8} einstein $s^{-1}\ cm^{-2}$ (6.94 mW cm^{-2}) and (3.54 ± 0.01) cm, respectively [24].

With the assistance of a thermostat (THD-2015, Tianheng, Ningbo, China), the temperature of the solutions in the photolysis experiments was maintained at (25 ± 0.5) °C. Phosphate (10 mM, for pH 5.0–8.0), borate (10 mM, for pH 8.0–10.5) and sodium hydroxide (10 mM, for pH 10.5–12.3) were used to buffer the solution pH. By purging with nitrogen gas (N_2, ≥99.99%), oxygen-free conditions in the photolysis experiments were achieved to minimize the interference of oxygen dissolved in the solutions. Initiated by UV irradiation at 253.7 nm, the photolysis experiments were conducted with the addition of *p*-BQ (40 μM, unless otherwise noted), CH_3OH (1.0 mM, unless otherwise noted), and MCAA (40 μM, unless otherwise noted) into the buffered solutions. At predetermined time intervals, the samples were withdrawn from the solutions. The analysis of the samples was carried out (always within 24 h) without quenching of residual *p*-BQ and CH_3OH, since the depletion of MCAA by *p*-BQ and CH_3OH was negligible. All experiments were independently conducted in duplicates or triplicates, and the average values along with standard deviation (±SD) were presented.

2.3. Analytical methods

Solution pH was detected by a pH meter, namely UB-7, Denver Instrument. An ion chromatograph (Dionex ICS-3000), which was equipped with a Dionex AS19 column (4 × 250 mm) and a Dionex AG19 guard column (4 × 50 mm), was used for the analysis of anions (chloride anion and monochloroacetate anion), with the suppressor current of 75 mA. The isocratic eluent of 30 mM KOH was set at a flow rate of 1.0 mL min^{-1}. *p*-BQ was analyzed by a Waters 1525 high performance liquid chromatography (HPLC), which was equipped with a Waters 2487 dual λ detector and a Waters symmetry C18 column (150 mm × 4.6 mm, 5 μm). The eluent of 0.1% acetic acid and methanol [90:10 (*v*/*v*)] at a flow rate of 1.0 mL min^{-1} was used for the HPLC analysis.

2.4. Computational details

The density functional theory (DFT) based theoretical calculations were carried out for the homogeneous gas-phase transformation of *p*-BQ in the presence of CH_3OH and H_2O without environmental effect. The theoretical results could help to thoroughly confirm the underlying mechanism for the acceleration of the e_{aq}^- generation from the *p*-BQ/UV process in aqueous solution with the addition of CH_3OH. Based on method B3LYP [32,33] with 6-311++G (3df,3pd) [34–36] basis set as implemented in the Gaussian 09 package [37], the geometrical parameters of the structures in the gas phase were optimized through density-functional theory (DFT) [38–40] (the ground states, the first triplet states and the transition states) and time-dependent density-functional theory (TDDFT) [41] (the first excited singlet states). The optimized structures of reactants, intermediates, transition states and products along the reaction paths are displayed in Fig. S1. The calculation of the energy of e_{aq}^- was via the optimization of the structures of the cage clusters of water $(H_2O)_6$ and $(H_2O)_6^-$ at the same level of theory [42], and the relative enthalpy of e_{aq}^- was calculated to be −2.6 kcal mol^{-1} [24]. The optimized structures of $(H_2O)_6$, $(H_2O)_6^-$, H_2O, OH^-, $ClCH_2COO^-$, $^{\bullet}CH_2COO^-$ and Cl^- could be seen in the previous research [24]. More details of the properties of structures are shown in the Supplementary Data (Text S1 and Table S1).

3. Results and discussion

3.1. Investigation of mechanism based on the theoretical calculations

3.1.1. Mechanism of photolysis at 253.7 nm in aqueous solution in the presence of CH_3OH

The photolysis of *p*-BQ (**A**) could induce the formation of *p*-HOC_6H_4OH (**E**) under UV irradiation at 253.7 nm in aqueous solution in the presence of CH_3OH [28], which was confirmed by the DFT based calculations. As shown in Scheme 1a, the consecutive formation of the first excited singlet state of *p*-BQ (**B**) (53.0 kcal mol^{-1}) and the first triplet state of *p*-BQ (**C**) (−2.4 kcal mol^{-1}) from **A** was induced by the photon absorption, and the formation of **C** was generated from **B** by intersystem crossing (−2.4 kcal mol^{-1}) [28]. The isolated **C** could induce the formation of *p*-benzosemiquinone radical (*p*-$HOC_6H_4O^{\bullet}$) (**D**) with the hydrogen donation of CH_3OH (−16.6 kcal mol^{-1}), competing with the quenching of **C** back to **A** (−50.6 kcal mol^{-1}) [28]. **E** could be generated from the disproportionation of **D** with the release of **A** (8×10^7 M^{-1} s^{-1}) [30], which was exothermic by 19.5 kcal mol^{-1}. As the product from the hydrogen abstraction of CH_3OH by **C** [28], $^{\bullet}CH_2OH$ hardly led the reduction of **A** to *p*-benzosemiquinone radical anion (*p*-$^{-}OC_6H_4O^{\bullet}$) (**D'**) [29] (the conjugate base of **D** with pK_a = 4.1) [43] (132.6 kcal mol^{-1}), which could be also converted back to **A** and **E** (−339.5 kcal mol^{-1}) [30]. The much more efficient reduction of **A** to **D'** could be achieved by $^{\bullet}CH_2O^{-}$ (−62.7 kcal mol^{-1}), which is the conjugate base of $^{\bullet}CH_2OH$ with pK_a = 10.7 [44]. The formation of **E** from the UV photolysis of **A** in the presence of CH_3OH [28] was thermodynamically feasible (Scheme 1a). The dominant step for the transformation in Scheme 1a was $\mathbf{C_1} \rightarrow \mathbf{C_2}$. The energy barrier of the transformation from $\mathbf{C_1}$ to $\mathbf{C_2}$ was calculated to be 3.7 kcal mol^{-1} with $\mathbf{TS_1}$ as the transition state. $\mathbf{TS_1}$ (201.83i cm^{-1}) was connected to $\mathbf{C_1}$ and $\mathbf{C_2}$, which was confirmed by the predicted vibrational frequencies and intrinsic reaction coordinate (IRC) calculation (Fig. 1a). Kinetically, the energy barrier of the dominant step for the formation of **E** from the UV photolysis of **A** in the presence of H_2O (2.4 kcal mol^{-1}) [25] was lower than that in the presence of CH_3OH in Scheme 1a (3.7 kcal mol^{-1}).

3.1.2. Mechanism of hydroxy-p-benzoquinone photolysis at 253.7 nm in aqueous solution in the presence of CH_3OH

As the primary product of the UV photolysis of *p*-BQ in aqueous solution [25], hydroxy-*p*-benzoquinone (**F**) could also induce the formation of **E** in the presence of CH_3OH and H_2O. As shown in Scheme 1b, **F** could induce the formation of benzene-1,2,4,5-tetraol (**F-E**), which could induce the reduction of **A** to **E** (−18.5 kcal mol^{-1}) [26]. The dominant step for the formation of **E** was the 1,4-addition reaction of **F-C** with H_2O [45,46], in which the nucleophilic addition of OH^{-} occurred at the α–β conjugated system of hydroxy-*p*-benzoquinone (from $\mathbf{F\text{-}C_1}$ to $\mathbf{F\text{-}C_2}$), followed by the protonation [45]. The energy barrier of the dominant step from $\mathbf{F\text{-}C_1}$ to $\mathbf{F\text{-}C_2}$ was calculated to be 5.6 kcal mol^{-1} with $\mathbf{TS_2}$ as the transition state. Moreover, the hydrogen abstraction of CH_3OH could be induced by **F-C** [28] at 1-position and 4-position, as shown in Scheme 1c and 1d. The generated semiquinone radicals ($\mathbf{F\text{-}D_2}$ and $\mathbf{F\text{-}D_3}$) could induce the reduction of **A** to **E** [45]. The energy barrier of the hydrogen abstraction of CH_3OH by **F-C** at 4-position (0.1 kcal mol^{-1} with $\mathbf{TS_4}$ as the transition state) was much lower than that at 1-position (14.0 kcal mol^{-1} with $\mathbf{TS_3}$ as the transition state), which could be interpreted by the steric effect [47] of the hydroxyl. The IRC calculation indicates that the transition states involving hydroxy-*p*-benzoquinone [i.e., $\mathbf{TS_2}$ (453.33i cm^{-1}), $\mathbf{TS_3}$ (628.07i cm^{-1}) and $\mathbf{TS_4}$ (106.91i cm^{-1})] were connected to their corresponding reactants and products (Fig. 1b–d).

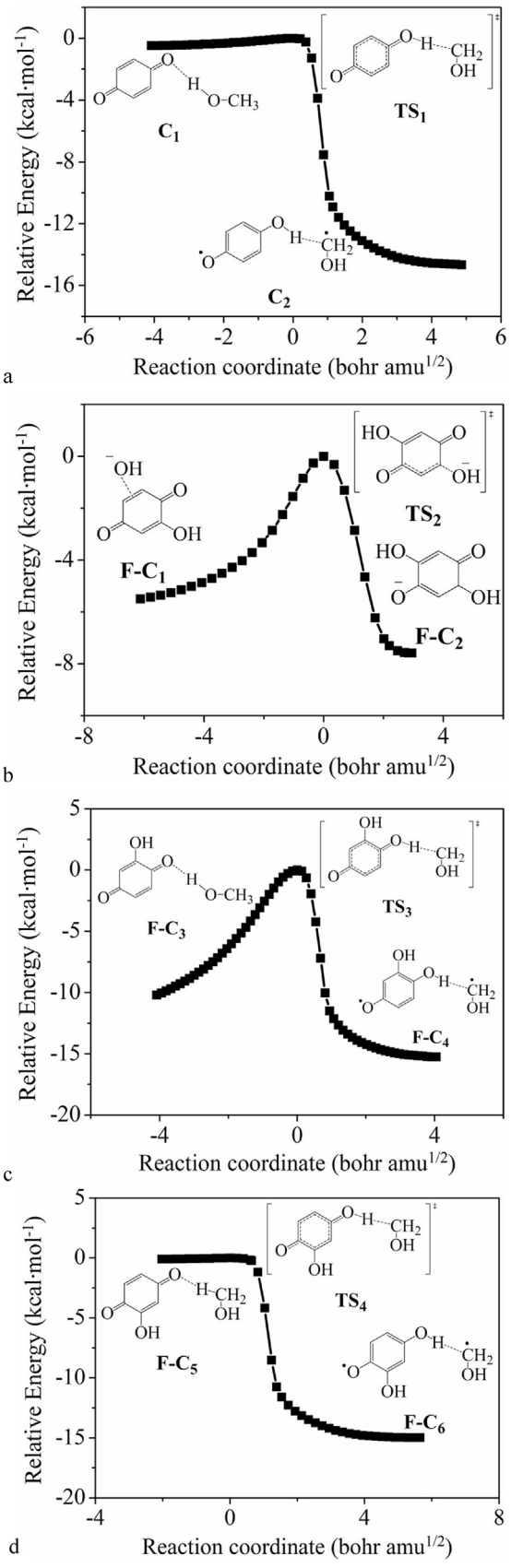

Fig. 1. (a) Energy profiles of minimum energy path (MEP) for the transformation from $\mathbf{C_1}$ to $\mathbf{C_2}$ in Scheme 1**a** calculated at the B3LYP/6-311++G (3df,3pd) level of theory. (b) Calculated MEP of reaction from $\mathbf{F\text{-}C_1}$ to $\mathbf{F\text{-}C_2}$ in Scheme 1**b**. (c) Calculated MEP of reaction from $\mathbf{F\text{-}C_3}$ to $\mathbf{F\text{-}C_4}$ in Scheme 1**c**. (d) Calculated MEP of reaction from $\mathbf{F\text{-}C_5}$ to $\mathbf{F\text{-}C_6}$ in Scheme 1**d**.

Consequently, the formation of p-HOC_6H_4OH from the UV photolysis of p-BQ in the presence of H_2O [26] was much more efficient than that in the presence of CH_3OH [28], which was confirmed by their respective energy barriers (2.4 kcal mol^{-1} for H_2O and 3.7 kcal mol^{-1} for CH_3OH). Comparatively, with the energy barrier of 0.1 kcal mol^{-1}, the hydrogen abstraction of CH_3OH by the first triplet state of hydroxy-p-benzoquinone at 4-position [28] was the major pathway for the formation of p-HOC_6H_4OH during the UV photolysis of hydroxy-p-benzoquinone in the presence of CH_3OH and H_2O, even though the first triplet state of hydroxy-p-benzoquinone could be efficiently quenched by H_2O to generate another two isomers of benzene-1,2,4,5-tetraol [**S-C** (at 3-position)

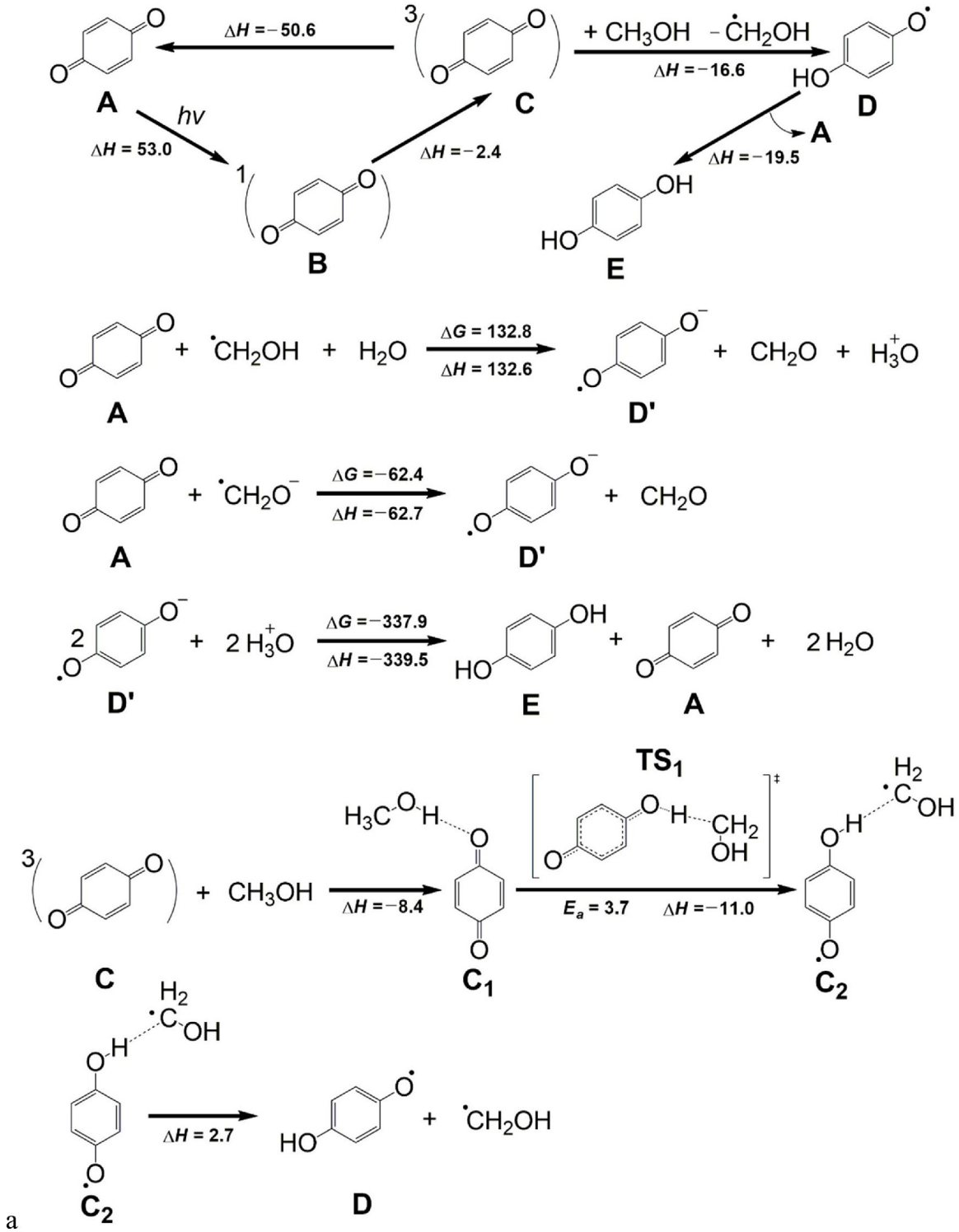

Scheme 1. Proposed pathways for the transformation of p-BQ under UV irradiation at 253.7 nm in aqueous solution in the presence of CH_3OH. (a) The formation of p-HOC_6H_4OH from p-BQ with the hydrogen donation of CH_3OH. (b) The formation of p-HOC_6H_4OH from hydroxy-p-benzoquinone with the hydrogen donation of H_2O. (c) The formation of p-$HOC_6H_4O^{\bullet}$ from the hydrogen abstraction of CH_3OH by hydroxy-p-benzoquinone at 1-position. (d) The formation of p-$HOC_6H_4O^{\bullet}$ from the hydrogen abstraction of CH_3OH by hydroxy-p-benzoquinone at 4-position. The energies (relative enthalpies and free energies) reported herein were calculated with zero-point energy (ZPE) correction and given in kcal·mol^{-1}.

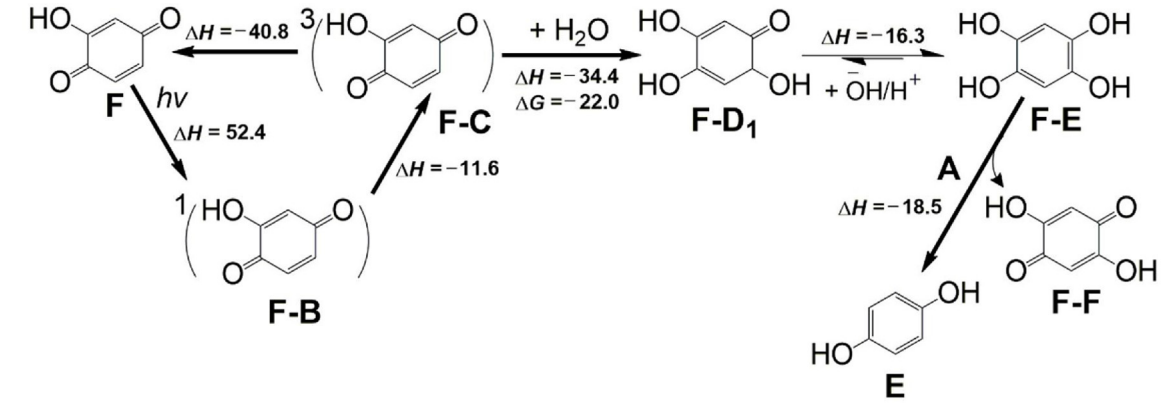

b

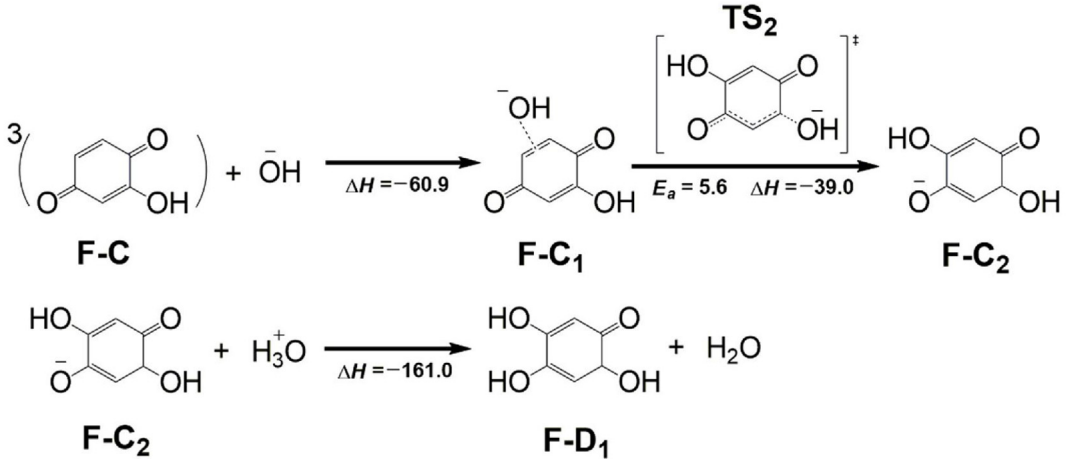

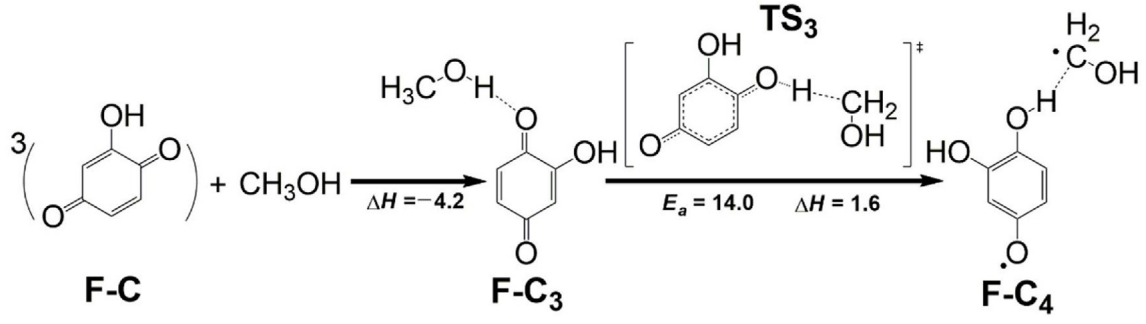

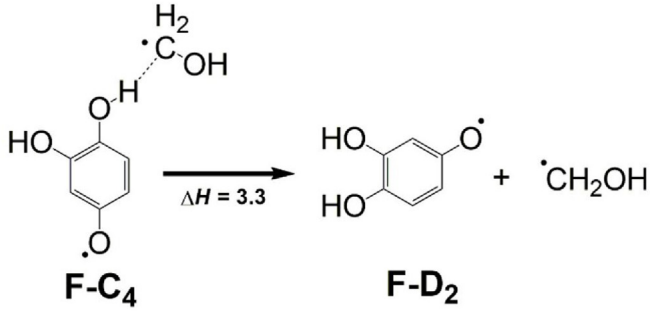

c

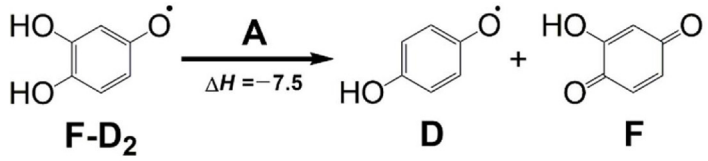

Scheme 1. (*Continued*)

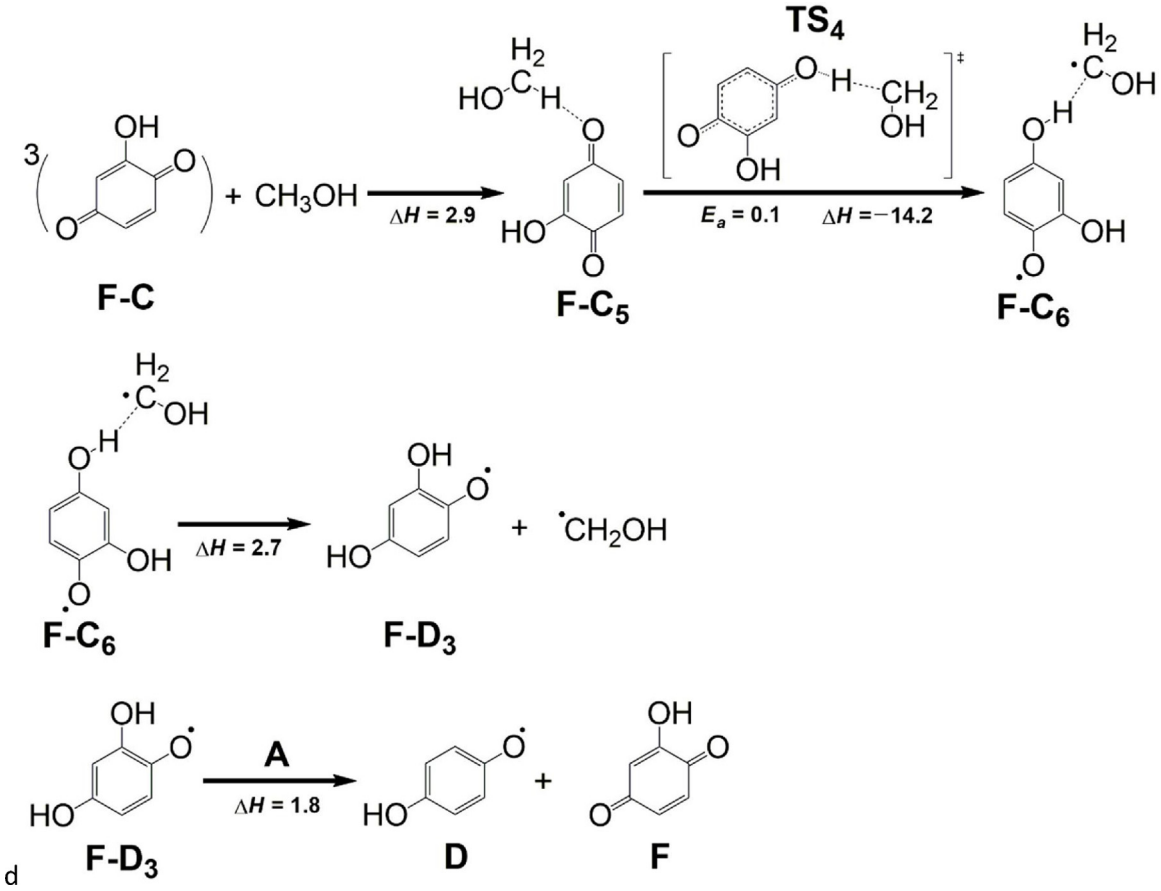

Scheme 1. (*Continued*)

and **S-E** (at 6-position) in Scheme S1] with the corresponding energy barriers of 0.3 kcal mol^{-1} and 1.6 kcal mol^{-1} (Text S1.2 and Scheme S1). Totally, with the catalysis of hydroxy-*p*-benzoquinone, CH_3OH could be the original source of e_{aq}^-, and *p*-HOC_6H_4OH was the primary intermediate for the generation of e_{aq}^- [25,27]. The generation of e_{aq}^- from *p*-HOC_6H_4OH was shown in detail in our recent study [25].

3.2. Generation of e_{aq}^- in the CH_3OH/*p*-BQ/UV process

Experimentally, the formation of e_{aq}^- generated in the CH_3OH/*p*-BQ/UV process was confirmed by monitoring the degradation of MCAA (the probe of e_{aq}^-) [17]. Fig. 2a shows the degradation of MCAA in the CH_3OH/*p*-BQ/UV process at pH 12.0, where *p*-hydroquinone exists in the forms of *p*-$HOC_6H_4O^-$ and *p*-$^-OC_6H_4O^-$ (Text S2 and Fig. S2a). In the preliminary studies, the negligible degradation of MCAA (40 μM, less than 3%) was observed in the presence of 40 μM *p*-BQ and 1.0 mM CH_3OH at pH 12.0 within 15 min without the UV irradiation. Similarly, it turned out that the degradation of MCAA (less than 6%) was insignificant in the presence of 1.0 mM CH_3OH at pH 12.0 within 15 min under the UV irradiation. In contrast, a higher degradation efficiency of MCAA (61%) with a pseudo-zero-order rate constant (*k*, μM min^{-1}) of (1.67 ± 0.04) μM min^{-1} was achieved within 15 min in the CH_3OH/*p*-BQ/UV process. Moreover, the degradation in the CH_3OH/*p*-BQ/UV process was much more efficient than that in the *p*-BQ/UV process, where 38% of MCAA [*k* = (1.00 ± 0.03) μM min^{-1}] was degraded within 15 min. Fig. 2b shows the similar decay of *p*-BQ in the two processes at pH 12.0. It could be interpreted by the respective energy barriers (2.4 kcal mol^{-1} for H_2O and 3.7 kcal mol^{-1} for CH_3OH) of the transformation of the first triplet state of *p*-BQ in the presence of CH_3OH and H_2O, which indicates that the presence of CH_3OH could not have a significant influence on the UV photolysis of *p*-BQ in aqueous solution. Thus, it could be concluded that the enhancement of the degradation efficiency might be induced by the extra reaction involving CH_3OH, namely the reaction of hydroxy-*p*-benzoquinone with CH_3OH.

Table 1
Rate constants (*k*) of MCAA (40 μM) degradation and chloride ion formation in the CH_3OH/*p*-BQ/UV process.

pH	Species	*k* (μM min^{-1})	R^2
5.8	MCAA	−0.1657 ± 0.0046	0.9955
	Cl^-	0.1608 ± 0.0037	0.9968
9.2	MCAA	−0.6238 ± 0.0036	0.9998
	Cl^-	0.6233 ± 0.0062	0.9994
12.0	MCAA	−1.7783 ± 0.0245	0.9989
	Cl^-	1.7760 ± 0.0253	0.9988

In the *p*-BQ/UV process, e_{aq}^- was the dominant reactive species responsible for the degradation. To confirm this primary reactive species in the CH_3OH/*p*-BQ/UV process, the mass balances of chlorine during the kinetic runs were determined at different pH. Fig. 2c shows that the degradation of MCAA was accompanied with the simultaneous formation of Cl^- in the process, and the invariable total chlorine (TCl) was also observed. The formation rates of chloride ion were further evaluated and displayed in Table 1, which were comparable to those of MCAA degradation at different pH, respectively. These results indicate that the degradation of MCAA was achieved via a reductive dechlorination process with the chlorine in MCAA being released as Cl^-.

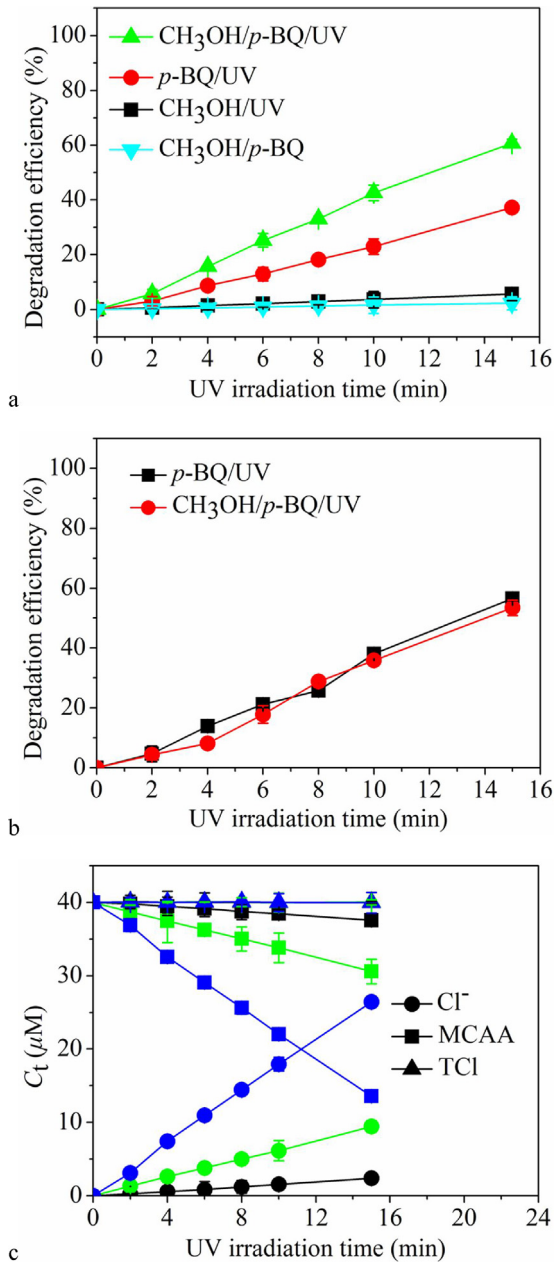

Fig. 2. (a) Degradation efficiency of MCAA (40 μM) in the *p*-BQ/UV process at pH 12.0 with and without the addition of CH_3OH. (b) Decay of *p*-BQ in the two processes at pH 12.0. (c) Total mass balances of chlorine (TCl) during the MCAA (40 μM) degradation in the CH_3OH/*p*-BQ/UV process at different pH [5.8 (black), 9.2 (green), 12.0 (blue)]. Total chlorine (TCl) was calculated by the equation of TCl = [MCAA] + [Cl^-], and the concentration of species was molar concentration. Error bars represent the standard deviation from triplicate experiments. (For interpretation of the references to colour in this figure legend, the reader is referred to the web version of this article).

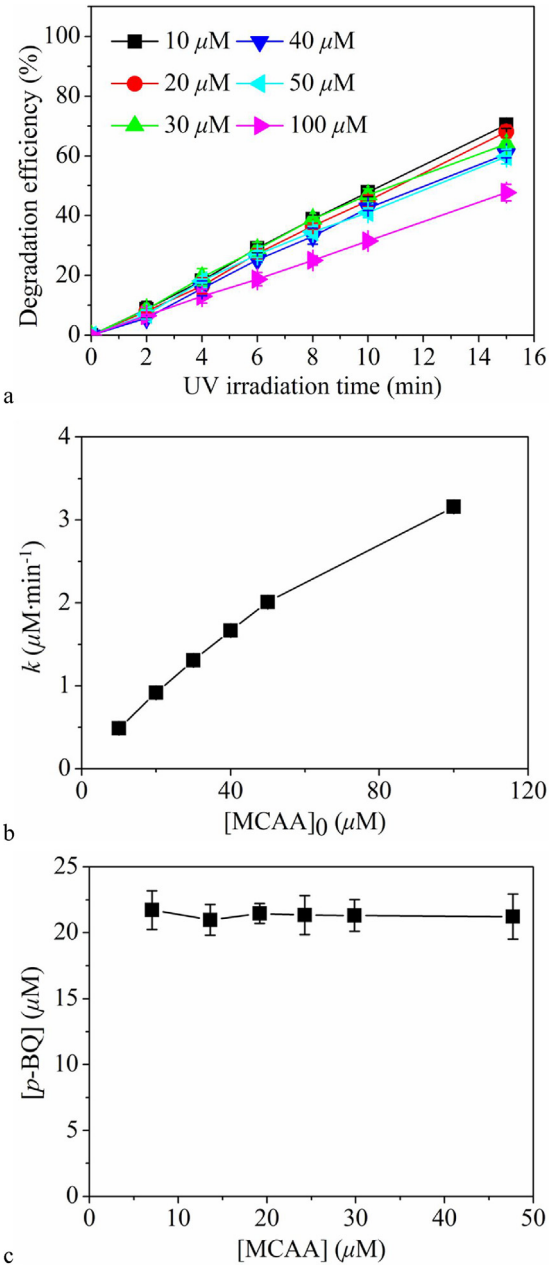

Fig. 3. (a) Influence of MCAA concentration (10–100 μM) on the degradation efficiency of MCAA in the CH_3OH/*p*-BQ/UV process at pH 12.0. (b) The degradation rate constants (*k*) versus the initial MCAA concentrations. (c) The relationship between the amounts of *p*-BQ and MCAA degraded in 15 min.

It has been reported that some other reactive species, e.g., H• (produced during rapid quenching of e_{aq}^- by H^+) [17], $•CH_2OH/•CH_2O^-$, semiquinone radical, could be also produced during the photoreactions of *p*-BQ in aqueous solution in the presence of CH_3OH [26,28]. H• (the standard reduction potential of about −2.3 V) [17], $•CH_2OH$ (−1.2 V) [48] and $•CH_2O^-$ (−2.5 V) [48] are more reductive than semiquinone radical (more than 0.0 V) [48], which strongly indicates that semiquinone radical could be excluded. Thermodynamically, $•CH_2OH$ and $•CH_2O^-$ preferred to induce the reduction of *p*-BQ to $p\text{-}^-OC_6H_4O•$ rather than induce the dechlorination of MCAA [Scheme 1a and reactions (S2–S3)]. Moreover, Cl^- release couldn't be observed from the degradation of MCAA by H•, since H• reacts with MCAA by abstracting H [17]. Consequently, as the primary reactive species, e_{aq}^- accounted for the MCAA degradation in the CH_3OH/*p*-BQ/UV process.

3.3. Influence of variables on the generation of e_{aq}^- in the CH_3OH/p-BQ/UV process

3.3.1. MCAA

Fig. 3a and b shows that with the concentration from 10 μM to 100 μM, the degradation efficiency of MCAA was positively dependent on the MCAA concentration at pH 12.0 in the process. The correlation indicates that higher initial concentration of MCAA could minimize the competing reactions of e_{aq}^- [49] to induce the higher degradation rate of MCAA. *p*-BQ and its derivatives might be the major competitors to lead to the side reactions of e_{aq}^- [50]. The

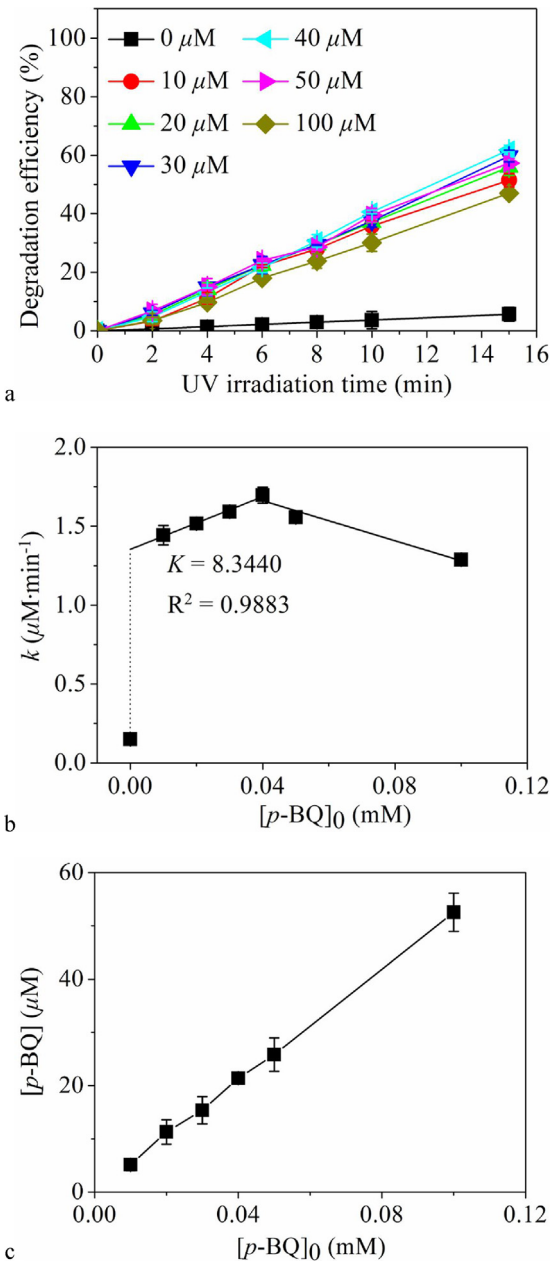

Fig. 4. (a) Influence of *p*-BQ concentration (0–100 μM) on the degradation efficiency of MCAA (40 μM) in the CH_3OH/*p*-BQ/UV process at pH 12.0. (b) (b) The degradation rate constants (*k*) versus the initial *p*-BQ concentrations. (c) The amount of *p*-BQ degraded in 15 min versus the initial *p*-BQ concentrations. The solid line indicates the best linear fit (b).

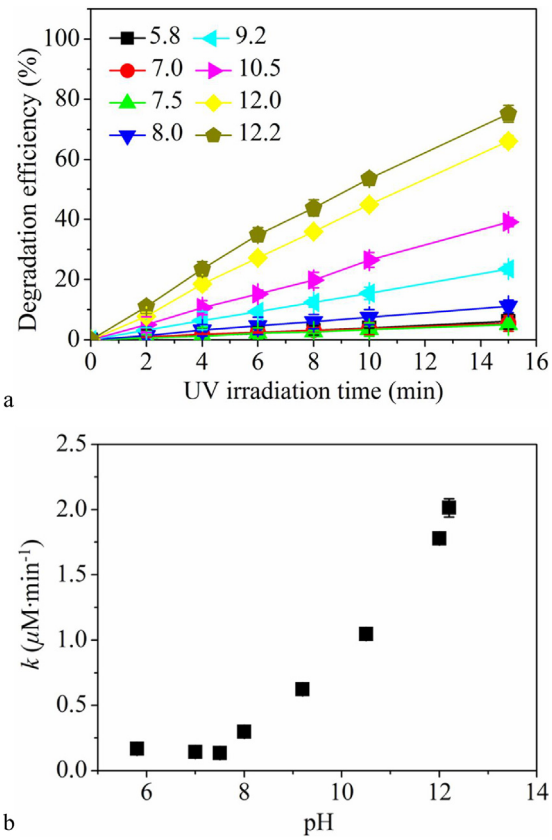

Fig. 5. (a) Influence of pH (5.8–12.2) on the degradation efficiency of MCAA (40 μM) in the CH_3OH/*p*-BQ/UV process. (b) The degradation rate constants (*k*) versus pH.

relationship between the amounts of *p*-BQ and MCAA degraded in 15 min was further investigated in Fig. 3c. The relationship in Fig. 3c indicates that the enhancement of the degradation of MCAA was independent of the transformation of *p*-BQ, which was consistent with the result in Fig. 2b. The enhancement might be induced by the addition of CH_3OH in the process, and more *p*-HOC_6H_4OH could be generated from the photoreaction of hydroxy-*p*-benzoquinone with CH_3OH, where hydroxy-*p*-benzoquinone acted as a catalyst (Scheme 1d).

3.3.2. *p*-BQ

Fig. 4a and b shows that the degradation of MCAA was enhanced by the increase of *p*-BQ concentration when the concentration was below 40 μM. The degradation rate was accelerated markedly from 0.1505 μM min^{-1} to 1.4432 μM min^{-1} by the addition of 10 μM *p*-BQ in the CH_3OH/UV process, and a further acceleration with the slope of $(8.3440 \pm 0.5226) \times 10^{-3}$ min^{-1} was observed from 10 to 40 μM. When the *p*-BQ concentration was above 40 μM, the residual *p*-BQ could quench e_{aq}^- efficiently (1.25×10^9 M^{-1} s^{-1}) [50], which induced the inhibition of the degradation of MCAA, as shown in Fig. 4b.

The results in Fig. 4c indicate that the transformation of *p*-BQ was positively dependent on the initial *p*-BQ concentration, which could induce the accumulation of hydroxy-*p*-benzoquinone [26]. Theoretically, with the catalysis of hydroxy-*p*-benzoquinone, the addition of CH_3OH in the process made it possible to generate more *p*-HOC_6H_4OH (Scheme 1d), which could eject more e_{aq}^- [25,27] to accelerate the degradation of MCAA. Moreover, it's obvious that the bulge in the degradation rate in Fig. 4b confirmed the synergistic effect of CH_3OH and *p*-BQ on the generation of e_{aq}^-.

3.3.3. pH

To confirm the influence of pH on the generation of e_{aq}^- in the process, the degradation efficiency of MCAA at different pH (5.8–12.2) was investigated in Fig. 5. As shown in Fig. 5a, the degradation was almost unchanged with pH from 5.8 to 7.5, followed by obvious promotion from 8.0 to 12.2. Fig. 5b further indicates the dependence of *k* on pH, which corroborated the tendency in Fig. 5a.

It has been reported that the solution pH might not have a significant influence on the transformation of *p*-BQ to *p*-HOC_6H_4OH with H_2O as the hydrogen donor in the *p*-BQ/UV process [25]. According to Scheme 1, the formation of *p*-$HOC_6H_4O^\bullet$ and $^\bullet CH_2OH$ with the hydrogen donation of CH_3OH was independent of pH. Since *p*-$^-OC_6H_4O^\bullet$ is the primary form of *p*-benzosemiquinone radical at pH from 5.8 to 12.2 (Text S2 and Fig. S2b), the effect of pH on the existence of *p*-$^-OC_6H_4O^\bullet$ could be excluded herein. While,

the solution pH plays an important role on the distribution molar ratio of $^{\bullet}CH_2OH$ and *p*-hydroquinone (Text S2 and Fig. S2a and S2c). As shown in Fig. S2c, $^{\bullet}CH_2OH$ is the dominant form at pH from 5.8 to 8.0, followed by the enhancement of the molar ratio of $^{\bullet}CH_2O^-$ with pH from 8.0 to 12.2. Since $^{\bullet}CH_2O^-$ (−2.5 V) [48] is much more reductive than $^{\bullet}CH_2OH$ (−1.2 V) [48], more generation of *p*-$^-OC_6H_4O^{\bullet}$ could be induced by the elevation of pH in the process. The preference for the reduction of *p*-BQ to *p*-$^-OC_6H_4O^{\bullet}$ by $^{\bullet}CH_2O^-$ could be also corroborated by the relative enthalpy difference in Scheme 1a. Then, more *p*-HOC_6H_4OH could be generated from *p*-$^-OC_6H_4O^{\bullet}$ with the increase of pH. Moreover, it has been reported that higher pH would promote the generation of e_{aq}^- from *p*-hydroquinone [25]. Thus, the dependence of *k* on pH could be explained by the facts described above, together with the generation of e_{aq}^- from the molecular *p*-hydroquinone (*p*-HOC_6H_4OH) via multiple site electron-proton transfer (MS-EPT) pathway [51] at pH below 8.0 [25]. Practically, the dependence of *k* on pH indicates that the CH_3OH/*p*-BQ/UV process may be favorable to be applied at strong alkaline conditions. Generally, electronegative substituents in the structures can increase the acidity of phenols [43], which may improve the e_{aq}^- generation from these phenols at neutral pH conditions. Thus, the UV photolysis of some quinones, which contain electronegative substituents in their structures, will be suitable for the treatment at neutral pH conditions.

3.3.4. CH_3OH

Theoretically, as the hydrogen donor [28], CH_3OH was the original reductant for the reduction of *p*-BQ to *p*-HOC_6H_4OH [28], which played a crucial role on the generation of e_{aq}^-. To experimentally confirm the role of CH_3OH in the process, the influence of CH_3OH concentration on the degradation of MCAA was investigated with the concentration from 0.0 mM to 2.5 mM at pH 12.0, as shown in Fig. 6a and b. The presence of 0.1 mM CH_3OH in the *p*-BQ/UV process could induce a similar bulge in the degradation rate from 1.0003 μM min^{-1} to 1.4868 μM min^{-1}, followed by a positive linear correlation with the CH_3OH concentration from 0.1 mM to 2.5 mM. The slope of the linear correlation was $(0.1799 \pm 0.0094) \times 10^{-3}$ min^{-1}, which indicates that the increase of CH_3OH concentration could not lead to efficient quenching of e_{aq}^- ($< 1.0 \times 10^4$ M^{-1} s^{-1}) [17]. The relationship in Fig. 6c further confirmed that the transformation of *p*-BQ in aqueous solution was almost independent of the addition of CH_3OH, which was consistent with the results in Figs. 2b and 3c.

Consequently, the significant role of CH_3OH on the generation of e_{aq}^- was experimentally demonstrated in Fig. 6a and b. The bulge in Fig. 6a and 6b could help to verify the synergistic effect of CH_3OH and *p*-BQ on the generation of e_{aq}^-. With the catalysis of hydroxy-*p*-benzoquinone, more addition of CH_3OH in the process could release more $^{\bullet}CH_2O^-$, which could induce more generation of the precursor of e_{aq}^- – *p*-HOC_6H_4OH [25,27]. This could explain the dependence on the CH_3OH concentration in Fig. 6a and 6b. Comparing the two linear correlations in Fig. 4b [the slope of $(8.3440 \pm 0.5226) \times 10^{-3}$ min^{-1}] and Fig. 6b [the slope of $(0.1799 \pm 0.0094) \times 10^{-3}$ min^{-1}], it's obvious that the e_{aq}^- generation efficiency was about 46 times more dependent on *p*-BQ than on CH_3OH, which indicates that *p*-BQ played a decisive role on the generation of e_{aq}^- in the CH_3OH/*p*-BQ/UV process.

3.4. Generation of e_{aq}^- in the $(R_1R_2R_3)COH$/*p*-BQ/UV process

The findings in the CH_3OH/*p*-BQ/UV process confirm that CH_3OH could induce the acceleration of the e_{aq}^- generation from the UV photolysis of *p*-BQ in aqueous solution, where CH_3OH acted as the hydrogen donor [28]. As the similar common alcohols [28], ethanol (CH_3CH_2OH) and 2-propanol [$(CH_3)_2CHOH$] might also induce the acceleration for the e_{aq}^- generation in the *p*-BQ/UV process, which was corroborated by Fig. 7a and b. As shown in Fig. 7a and b, the similar degradation efficiency of MCAA was observed in the $(R_1R_2)CHOH$/*p*-BQ/UV process. As the similarity of the three alcohols, the α-H is the key factor to the acceleration in the processes [28], which was supported by Fig. 7c. As an alcohol without the α-H, *tert*-butanol [$(CH_3)_3COH$] didn't accelerate the e_{aq}^- generation in the *p*-BQ/UV process.

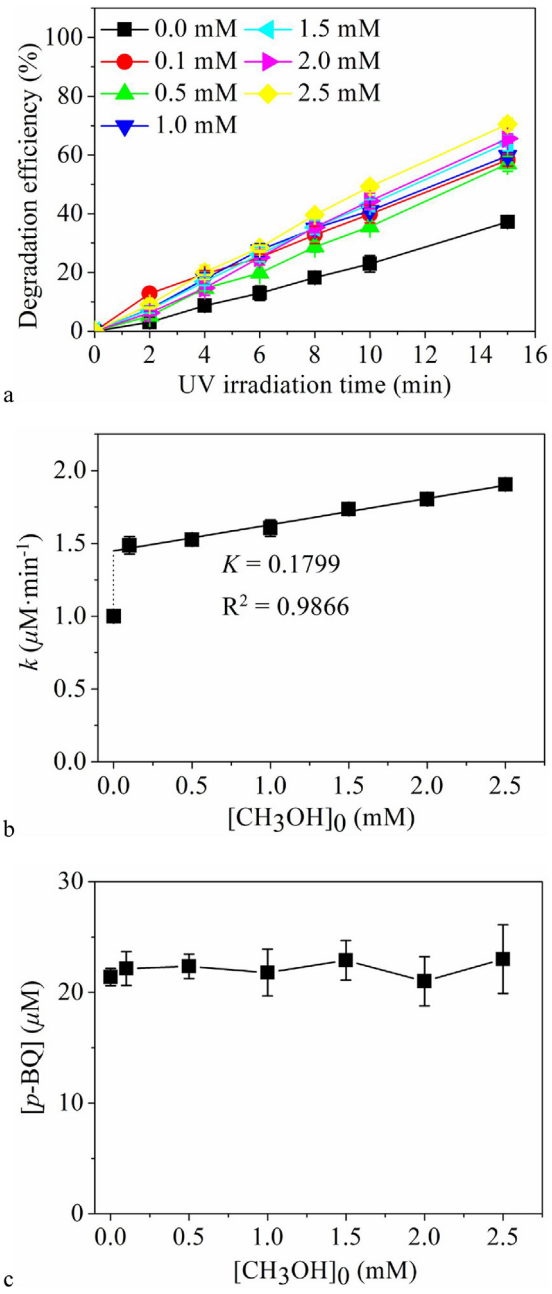

Fig. 6. (a) Influence of CH_3OH concentration (0.0–2.5 mM) on the degradation efficiency of MCAA (40 μM) in the CH_3OH/*p*-BQ/UV process at pH 12.0. (b) The degradation rate constants (*k*) versus the initial CH_3OH concentrations. (c) The amount of *p*-BQ degraded in 15 min versus the initial CH_3OH concentrations. The solid line indicates the best linear fit (b).

4. Conclusions

This present work has investigated the acceleration of the e_{aq}^- generation from the *p*-BQ/UV process in aqueous solution with the addition of CH_3OH, and the underlying mechanism was the-

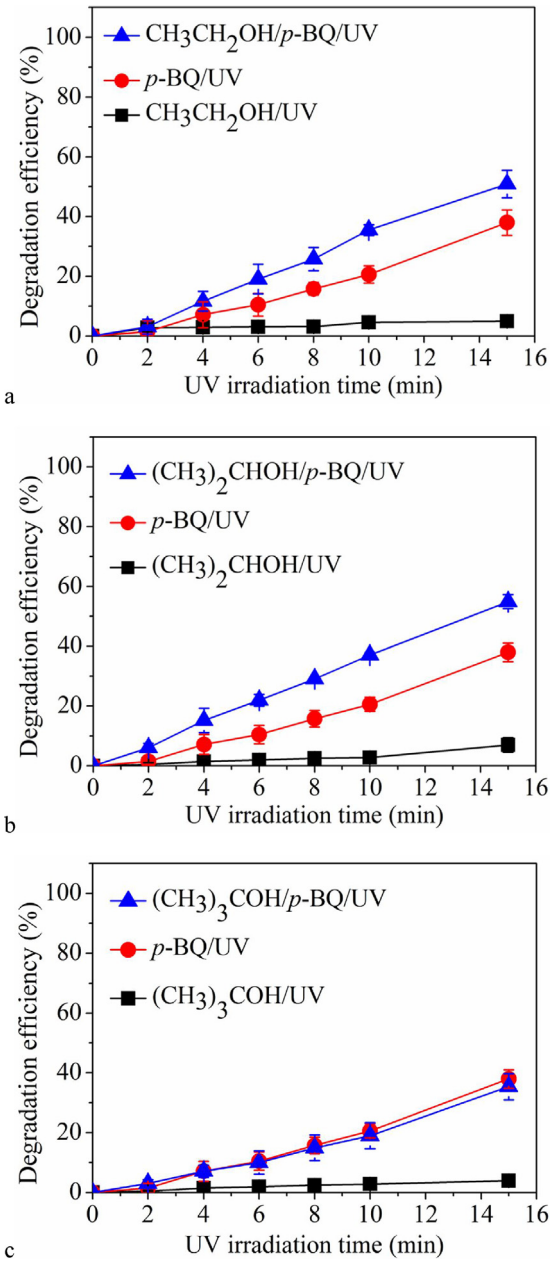

Fig. 7. Degradation efficiency of MCAA (40 μM) in the *p*-BQ/UV process at pH 12.0 with and without the addition of $(R_1R_2R_3)COH$ [(a) CH_3CH_2OH, (b) $(CH_3)_2CHOH$, and (c) $(CH_3)_3COH$] (1.0 mM).

oretically confirmed. Theoretically, the formation of *p*-HOC_6H_4OH from the UV photolysis of *p*-BQ in the presence of H_2O [26] was almost independent of the addition of CH_3OH. With hydroxy-*p*-benzoquinone (the primary product of the UV photolysis of *p*-BQ in the process) [25] as the photocatalyst, the reduction of *p*-BQ to *p*-HOC_6H_4OH could be induced by CH_3OH, which was much more efficient than that by H_2O. The enhanced reduction of *p*-BQ in the case of CH_3OH could account for the acceleration of the e_{aq}^- generation in the CH_3OH/*p*-BQ/UV process.

Overall, the enhancement of the e_{aq}^- generation in the *p*-BQ/UV process induced by the alcohols indicates the importance of the hydrogen donation in the process [28]. The findings in this study make it possible to induce the e_{aq}^- generation from the UV photolysis of quinones in the presence of alcoholic groups with the α-H, since the widely distributed natural organic matters (NOM) usually contain quinone-like groups [52,53], as well as alcoholic groups [54]. These processes will be much more environmentally friendly to generate e_{aq}^- for the pollution remediation. The mechanism investigated in this study will also help to strengthen the understanding of the transformation of quinones under UV irradiation in aqueous solution in the presence of alcohols with the α-H [28].

Acknowledgements

This work was financially supported by the National Natural Science Foundation of China (Grant No. 51378141 and 21203042), the Fundamental Research Funds for the Central Universities (Grant No. HIT. NSRIF. 2013057), the Scientific Research Foundation of Heilongjiang Province for Postdoctors (LBH-Q15057), the Funds of the State Key Laboratory of Urban Water Resource and Environment (HIT, 2016DX04, 2016DX13 and 2016TS02), the Foundation for the Author of National Excellent Doctoral Dissertation of China (201346), the Fundamental Research Funds for the Central Universities of China (AUGA5710056314), the Heilongjiang Province Science Foundation for General Program (E201427), and the Open Projects of Key Laboratory of Polyoxometalate Science of Ministry of Education (NENU) and State Key Laboratory of Supramolecular Structure and Materials (JLU) (SKLSSM201723).

Appendix A. Supplementary data

Supplementary data associated with this article can be found, in the online version, at http://dx.doi.org/10.1016/j.apcatb.2017.07.031.

References

[1] B.P. Vellanki, B. Batchelor, A. Abdel-Wahab, Environ. Eng. Sci. 30 (5) (2013) 264–271.
[2] X. Li, J. Ma, G. Liu, J. Fang, S. Yue, Y. Guan, L. Chen, X. Liu, Environ. Sci. Technol. 46 (13) (2012) 7342–7349.
[3] X. Liu, S. Yoon, B. Batchelor, A. Abdel-Wahab, Sci. Total Environ. 454–455 (2013) 578–583.
[4] X. Liu, S. Yoon, B. Batchelor, A. Abdel-Wahab, Chem. Eng. J. 215–216 (2013) 868–875.
[5] X. Liu, B.P. Vellanki, B. Batchelor, A. Abdel-Wahab, Chem. Eng. J. 237 (2014) 300–307.
[6] B. Jung, R. Nicola, B. Batchelor, A. Abdel-Wahab, Chemosphere 117 (2014) 663–672.
[7] Z. Song, H. Tang, N. Wang, L. Zhu, J. Hazard. Mater. 262 (2013) 332–338.
[8] Y. Qu, C. Zhang, F. Li, J. Chen, Q. Zhou, Water Res. 44 (9) (2010) 2939–2947.
[9] Y. Qu, C.-J. Zhang, P. Chen, Q. Zhou, W.-X. Zhang, Chemosphere 107 (2014) 218–223.
[10] Y. Wang, P. Zhang, J. Environ. Sci. 26 (11) (2014) 2207–2214.
[11] C. Zhang, Y. Qu, X. Zhao, Q. Zhou, Clean–Soil Air Water 43 (2) (2015) 223–228.
[12] B.P. Vellanki, B. Batchelor, J. Hazard. Mater. 262 (2013) 348–356.
[13] J. Fu, Z.-M. Zhang, J.-Y. Tang, Q.-F. Zeng, S.-Q. An, H.-L. Zhu, J. Environ. Eng.–ASCE 136 (11) (2010) 1314–1319.
[14] M. Fischer, P. Warneck, J. Phys. Chem. 100 (37) (1996) 15111–15117.
[15] L. Khriachtchev, M. Pettersson, E. Isoniemi, M. Räsänen, J. Chem. Phys. 108 (14) (1998) 5747–5754.
[16] C.A. Linkous, C. Huang, J.R. Fowler, J. Photochem. Photobiol. A: Chem. 168 (3) (2004) 153–160.
[17] G.V. Buxton, C.L. Greenstock, W.P. Helman, A.B. Ross, J. Phys. Chem. Ref. Data 17 (2) (1988) 513–886.
[20] P. Calza, E. Pelizzetti, J. Photochem. Photobiol. A: Chem. 162 (2–3) (2004) 609–613.
[21] H. Park, C.D. Vecitis, J. Cheng, N.F. Dalleska, B.T. Madere, M.R. Hoffmann, Photochem. Photobiol. Sci. 10 (12) (2011) 1945–1953.
[22] L.I. Grossweiner, G.W. Swenson, E.F. Zwicker, Science 141 (3583) (1963) 805–806.
[23] H.-I. Joschek, L.I. Grossweiner, J. Am. Chem. Soc. 88 (14) (1966) 3261–3268.
[24] J. Gu, J. Ma, J. Jiang, L. Yang, J. Yang, J. Zhang, H. Chi, Y. Song, S. Sun, W.Q. Tian, Appl. Catal. B.: Environ. 200 (2017) 585–593.
[25] J. Gu, L. Yang, J. Ma, J. Jiang, J. Yang, J. Zhang, H. Chi, Y. Song, S. Sun, W.Q. Tian, Appl. Catal. B.: Environ. 212 (2017) 150–158.
[26] H. Görner, J. Phys. Chem. A 107 (51) (2003) 11587–11595.
[27] H.-I. Joschek, S.I. Miller, J. Am. Chem. Soc. 88 (14) (1966) 3273–3281.
[28] H. Görner, J. Phys. Chem. A 111 (15) (2007) 2814–2819.
[29] P. Neta, J. Grodkowski, A.B. Ross, J. Phys. Chem. Ref. Data 25 (3) (1996) 709–1050.

[30] V.A. Roginsky, L.M. Pisarenko, W. Bors, C. Michel, J. Chem. Soc. Perkin Trans. 2 (4) (1994) 871–876.
[31] C.H. Jo, A.M. Dietrich, J.M. Tanko, Water Res. 45 (8) (2011) 2507–2516.
[32] C. Lee, W. Yang, R.G. Parr, Phys. Rev. B 37 (2) (1988) 785–789.
[33] A.D. Becke, J. Chem. Phys. 98 (7) (1993) 5648–5652.
[34] A.D. McLean, G.S. Chandler, J. Chem. Phys. 72 (10) (1980) 5639–5648.
[35] R. Krishnan, J.S. Binkley, R. Seeger, J.A. Pople, J. Chem. Phys. 72 (1) (1980) 650–654.
[36] M.J. Frisch, J.A. Pople, J.S. Binkley, J. Chem. Phys. 80 (7) (1984) 3265–3269.
[37] M.J. Frisch, G.W. Trucks, H.B. Schlegel, G.E. Scuseria, M.A. Robb, J.R. Cheeseman, et al., Gaussian 09, Revision A.02, Gaussian, Inc, Wallingford, CT, 2009.
[38] P. Hohenberg, W. Kohn, Phys. Rev. 136 (3B) (1964) B864–B871.
[39] W. Kohn, L.J. Sham, Phys. Rev. 140 (4A) (1965) A1133–A1138.
[40] R.G. Parr, W. Yang, Oxford University Press: New York, 1989.
[41] R.E. Stratmann, G.E. Scuseria, M.J. Frisch, J. Chem. Phys. 109 (19) (1998) 8218–8224.
[42] I.I. Zakharov, J. Struct. Chem. 55 (1) (2014) 1–7.
[43] J.J. Warren, T.A. Tronic, J.M. Mayer, Chem. Rev. 110 (12) (2010) 6961–7001.
[44] M. Simic, P. Neta, E. Hayon, J. Phys. Chem. 78 (11) (1969) 3794–3800.
[45] M. Uchimiya, A.T. Stone, Chemosphere 77 (4) (2009) 451–458.
[46] J.A. Perlinger, V.M. Kalluri, R. Venkatapathy, W. Angst, Environ. Sci. Technol. 36 (12) (2002) 2663–2669.
[47] M. Alipour, Chem. Phys. 434 (2014) 11–14.
[48] P. Wardman, J. Phys. Chern. Ref. Data 18 (4) (1989) 1637–1755.
[49] W.M. Draper, D.G. Crosby, J. Agric. Food Chem. 31 (4) (1983) 734–737.
[50] E.J. Hart, S. Gordon, J.K. Thomas, J. Phys. Chem. 68 (6) (1964) 1271–1274.
[51] D.R. Weinberg, C.J. Gagliardi, J.F. Hull, C.F. Murphy, C.A. Kent, B.C. Westlake, A. Paul, D.H. Ess, D.G. McCafferty, T.J. Meyer, Chem. Rev. 112 (7) (2012) 4016–4093.
[52] S. Kang, W. Choi, Environ. Sci. Technol. 43 (3) (2009) 878–883.
[53] M. Fujii, A. Imaoka, C. Yoshimura, T.D. Waite, Environ. Sci. Technol. 48 (8) (2014) 4414–4424.
[54] J. Chen, B. Gu, E.J. LeBoeuf, H. Pan, S. Dai, Chemosphere 48 (1) (2002) 59–68.

Further reading

[18] D.H. Paik, I.-R. Lee, D.-S. Yang, J.S. Baskin, A.H., Zewail, 2004. Science, 306(5696), 672-675.

[19] A.E. Bragg, J.R.R. Verlet, A. Kammrath, O. Cheshnovsky, D.M. Neumark, 2005. J. Am. Chem. Soc., 127(43), 15283-15295.